DEPTH-INDEPENDENT NARROW BEAMWIDTH 3D ULTRASONIC IMAGE FORMATION TECHNIQUE

Zalman M. Benenson, Alexey B. Elizarov, Tatiana V. Yakovleva
Scientific Council on Cybernetics, Russian Academy of Sciences,
Vavilova st. 40, Moscow, 119991, Russia
William D. O'Brien, Jr.
Bioacoustics Research Laboratory, Department of Electrical and Computer Engineering, University of Illinois,
405 N. Mathews, Urbana IL 61801 U.S.A.

Abstract – A technique is proposed that generates a depth-independent and narrow beamwidth 3D ultrasonic image. A high-frequency, wide-bandwidth spherical transducer is scanned in 2D along Cartesian coordinates. The received wideband ultrasonic pulses are dynamically focused by means of correcting the spatial spectrum of signals for various temporal frequencies. The main procedures of the algorithm consist in the direct and inverse fast Fourier transforms by time and by two spatial Cartesian coordinates.

I. INTRODUCTION

In, for example, ophthalmology, dermatology and mammography, it is highly desirable to have very high lateral and axial resolutions that are used for 3D image formation. These high resolutions can be achieved at high frequencies, namely, from 20 MHz to 100 MHz, but, at the present time, it is challenging to fabricate a phased array transducer at such frequencies, especially a 2D phased array. In this paper, an approach is considered that is based on a one-element transmit-receive transducer with a large aperture and fixed focal distance that moves in Cartesian coordinates (x,y) in the plane $z=0$ (Fig.1).

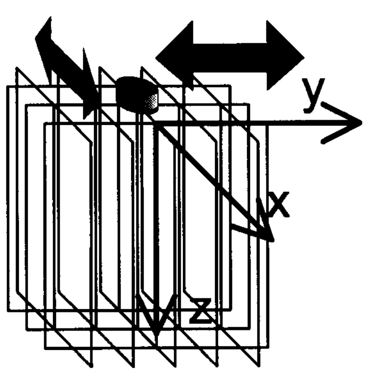

Fig. 1. Scheme of scanning.

In the literature various dynamic focusing strategies are considered for such a scanning scheme, for instance [1]. The approach developed herein is based on the theoretical estimations of the 2D Fourier transform of the transmit and receive radiation patterns, and assuming the Born approximation. The analysis of these estimations allows for the development of the algorithms based on the 3D fast Fourier transform. The paper proposes a theory for developing 3D dynamic focusing algorithms as well as providing results about their mathematical and physical experiments. These algorithms can be efficiently implemented in modern fast signal processing devices. The results of the work show that in 3D space a depth-independent narrow beamwidth can be synthesized.

II. THEORY

The Fourier transform of the transmit radiation pattern for the signal emitted by an aperture mounted in a rigid baffle is expressed as [2]:

$$u_{tr}\left(\Omega_x,\Omega_y,\omega,z\right)=u_0\left(\Omega_x,\Omega_y,\omega\right)\times \times\left[\frac{\exp\left(iz\sqrt{\left(\frac{\omega}{c_0}\right)^2-\Omega_x^2-\Omega_y^2}\right)}{\sqrt{1-\frac{\Omega_x^2+\Omega_y^2}{\left(\omega/c_0\right)^2}}}\right] \quad (1)$$

where $u_0\left(\Omega_x,\Omega_y,\omega\right)$ is the Fourier transform of the aperture-lens function in the x-y plane by the Cartesian coordinates (x,y); Ω_x, Ω_y are the spatial frequencies, ω is the temporal frequency, and c_0 is the sound speed. The Fourier transform of the receive radiation pattern by the same aperture-lens combination is [2]:

$$u_{re}\left(\Omega_x,\Omega_y,\omega,z\right)=u_0\left(\Omega_x,\Omega_y,\omega\right)\times \times\exp\left(iz\sqrt{\left(\frac{\omega}{c_0}\right)^2-\Omega_x^2-\Omega_y^2}\right). \quad (2)$$

It can be shown [2] for the monopole scattering case, and assuming the Born approximation, that the Fourier transform of the received signal at the output of the moving transducer is:

$$\tilde{V}_{re}\left(\Omega_x,\Omega_y,\omega,z\right)=K_1V\left(\omega\right)f_2\left(\omega\right)\frac{\omega^2}{c_0^2}\times \times u\left(\Omega_x,\Omega_y,\omega,z\right)\Gamma\left(\Omega_x,\Omega_y,z\right), \quad (3)$$

where K_1 is a scale coefficient, $V(\omega)$ is the Fourier transform of the vibrating velocity on the transmit aperture, $f_2(\omega)$ is the Fourier transform of the pulse response function of the receive aperture,

$$u\left(\Omega_x,\Omega_y,\omega,z\right)=\iint u_{tr}\left(\Omega_x',\Omega_y',\omega,z\right)\times \times u_{re}\left(\Omega_x-\Omega_x',\Omega_y-\Omega_y',\omega,z\right)d\Omega_x'd\Omega_y', \quad (3a)$$

and $\Gamma\left(\Omega_x,\Omega_y,z\right)$ is the Fourier transform of some function of the scattering medium $\gamma(x,y,z)$.

It is assumed that the scan lengths of the transducer's trajectory along x- and y-coordinates are sufficiently large.

Mathematical simulation and physical experiment for a rectangular transducer with a fixed focal point and a Gaussian apodization function are presented. Also, a spherical transducer is considered.

In the first case, *i.e.* for the Gaussian apodization function, the following expression is valid for the function $u(\bullet)$:

$$u^G\left(\Omega_x,\Omega_y,\omega,z\right)=K_2\exp\left(-\frac{\alpha+i\zeta}{2}\left(\Omega_x^2+\Omega_y^2\right)\right)\times \times\exp\left(2iz\frac{\omega}{c_0}\right) \quad (4)$$

where

$$\alpha=\frac{1}{4\left(\frac{1}{a^2}+\frac{\omega^2}{c_0^2}\frac{a^2}{4F^2}\right)},\qquad \zeta=\frac{c_0}{2\omega}z+\zeta_0,$$

$$\zeta_0=-\frac{c_0}{2\omega}\frac{F}{1+4\frac{c_0^2}{\omega^2}\frac{F^2}{a^4}}, \quad (4a)$$

$2a$ is the aperture size, and F is the focal distance.

The expression for ζ is known *a priori*. Multiplying (4) by $\exp\left(i\frac{\zeta}{2}\left(\Omega_x^2+\Omega_y^2\right)\right)$ yields the Fourier transform of the resulting radiation pattern: $\exp\left(-\frac{\alpha}{2}\left(\Omega_x^2+\Omega_y^2\right)\right)$. Correspondingly, the radiation pattern can be expressed by $L(x,y,\omega)=\exp\left(-\frac{x^2+y^2}{2\alpha}\right)$. This means that the lateral resolution δl for the Gaussian beam of the moving aperture is the same at all values of the depths z; that is, it is depth independent, starting from the zone near the transducer's surface. Thus, $\delta l\approx\frac{2F\lambda}{\pi 2a}$ at the -6 dB level, where λ is the wavelength. It is assumed that the aperture size is much larger than the wavelength.

Based on (4) the following algorithm was then developed for processing a set of received signals obtained from the moving transducer as a function of the transducer's coordinates x and y.

(1) Fast Fourier transform (FFT) of the received signals by time t.

(2) FFT by coordinates x and y.

(3) Interpolate the 3D data array from step (2) to a new regular grid with coordinates $\left(\Omega_x,\Omega_y,\tilde{\omega}\right)$, where $\tilde{\omega}=\omega+\frac{c_0^2}{8\omega}\left(\Omega_x^2+\Omega_y^2\right)$. Then, multiply the interpolated data by the factor $\exp\left(i\zeta_0\omega(\tilde{\omega})\right)$.

(4) Inverse 3D FFT the result of step (3) by $\left(\Omega_x,\Omega_y,\tilde{\omega}\right)$.

(5) Calculate the magnitude of analytical spatial-temporal data set to obtain the 3D image.

The operations in steps (3) and (4) correspond to multiplying the result of step (2) by the focusing term $\exp\left(i\zeta(\omega,z)\left(\Omega_x^2+\Omega_y^2\right)\right)$ and inverse 3D Fourier transforming by $(\Omega_x, \Omega_y, \omega)$ all values of z simultaneously.

III. MATHEMATICAL SIMULATION FOR THE CASE OF THE GAUSSIAN APODIZATIONFUNCTION

The algorithm described above was simulated on a PC. In the model, spatial distribution of the point reflectors was included. The reflectors were separated spatially from 0.2 cm to 6 cm. The central frequency of the transmit pulse was 7.5 MHz with a bandwidth of 5 MHz. The transducer's aperture size was $2a = 1.2$ cm and the focal distance $F = 1.8$ cm. The Gaussian apodization function was dropped to zero at the level of -8 dB at the aperture edges. The transmitted and received signals were calculated from the Green's function of the Helmholtz equation. The transducer's aperture was mounted in a rigid baffle.

Fig. 2 illustrates the simulation results for the distances $z = 0.3$ cm and $z = 6.0$ cm. The same figure shows the corresponding cross sections that demonstrate the depth independence of the beamwidth for quite a large depth interval. It is interesting to note that the beamwidth near the aperture is less than the aperture size.

IV. RESULTS FOR THE SPHERICAL TRANSDUCER

For the spherical transducer of the curvature radius F and aperture diameter $2a$, the Fourier transform of the function of initial conditions $u_0(\bullet)$ (to be used in (1) and (3)) is:

$$u_0(\Omega_x, \Omega_y, \omega) = \int_0^a r dr \exp\left(-\frac{i\omega r^2}{c_0 2F}\right) J_0\left(r\sqrt{\Omega_x^2 + \Omega_y^2}\right) \quad (5)$$

where $r = \sqrt{x^2 + y^2}$, and J_0 is a Bessel function.

The convolution of the Fourier transforms of radiation patterns (1) and (3) $u^{(s)}$, taking into account (5), was computed. The magnitude $A^{(s)}$ and the phase φ of $u^{(s)}(\bullet)$ are presented in Fig. 3 as functions of $\Omega = \sqrt{\Omega_x^2 + \Omega_y^2}$ for $f = 5$ MHz, $F = 8.0$ cm, and $2a = 2.5$ cm.

The expression for $u^{(s)}$ is approximated by:

$$u^{(s)}(\Omega_x, \Omega_y, \omega, z) \approx A^{(s)}(\Omega, \omega, z) \times \\ \times \exp\left(i\psi_1(z - F)\psi_2\left(\frac{c_0}{2\omega}\Omega\right)\right)\exp\left(i2\frac{\omega}{c_0}z\right) \quad (6)$$

where $\Omega = \sqrt{\Omega_x^2 + \Omega_y^2}$, and ψ_1 and ψ_2 are piece-linear functions. The positive function $A^{(s)}(\bullet)$ can be approximated by the rectangular function at $z < F$ and by the Gaussian function at $z > F$.

As one can see from Fig. 3, the width of the function A is approximately constant over large depth intervals and, consequently, the radiation pattern width does not substantially change with

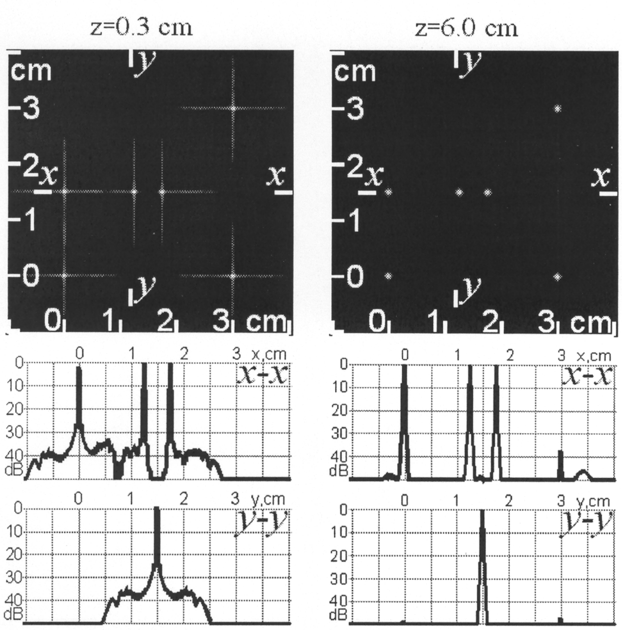

Fig. 2. Simulation results. Dynamic range 50 dB.

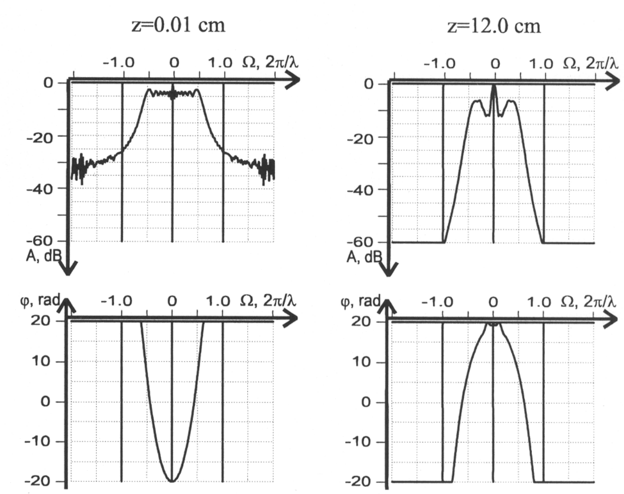

Fig. 3. Graphs of magnitude and phase of $u^{(s)}$.

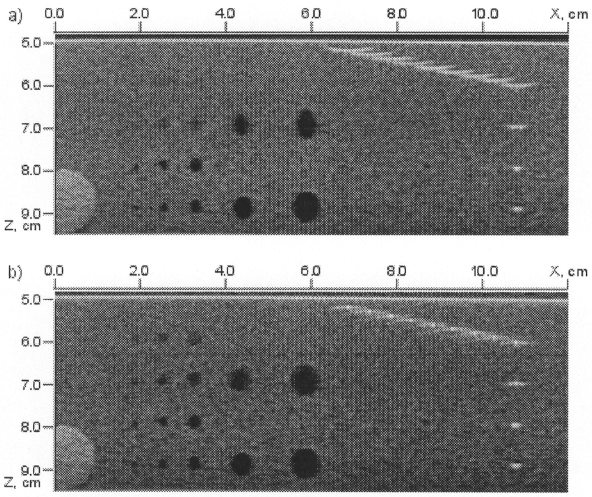

Fig. 4. Phantom image. a) before processing; b) after processing; dynamic range 70 dB.

distance if the transducer is moved along the coordinates x and y over sufficiently long trajectories. The signal processing algorithm is approximately the same as in section II; however, the Fourier transform by time is implemented for a few depth intervals in order to take into account the piece-linearity of the functions ψ_1 and ψ_2 contained in the expressions for the phase.

We have conducted the simulation of the algorithm for spherical transducers for a few variants of parameters:

1) $f = 15$ MHz, $2a = 1.0$ cm, $F = 2.0$ cm. The lateral resolution was 0.25 mm and the axial resolution was 0.1 mm.

2) $f = 5$ MHz, $2a = 2.5$ cm, $F = 8.0$ cm. The lateral resolution was 0.9 mm and the axial resolution was 0.3 mm.

V. THE RESULTS OF THE PHYSICAL EXPERIMENT

To verify the simulated results, a physical experiment was conducted. In order to decrease the experiment duration the scanning was implemented only in the x-axis direction. A spherical transducer was used with $f = 5$ MHz, bandwidth 1.5 MHz, $F = 8.0$ cm, and $2a = 2.5$ cm. The phantom (Model 539, ATS Laboratories Inc., Bridgeport CT) was positioned in a temperature-controlled degassed water tank.

Fig. 4 illustrates the results of the experiment before and after the signal processing. The lateral resolution is approximately the same in front and behind the focal point and corresponds to its theoretical estimation $\delta l = \dfrac{\lambda F}{2a \cdot 1.5} = 0.064$ cm. The side lobes were between -12 dB and -18 dB. Such a high side lobe level can be explained by the fact that the Fourier transform of the radiation pattern is a function of $\sqrt{\Omega_x^2 + \Omega_y^2}$, while in the experiment it was possible only to calculate the Fourier transform of the signal as a function of Ω_x. That is why the influence of the y-coordinate led to the side lobe level increase.

VI. CONCLUSION

The proposed methodology of 3D acoustic image formation based on fast 3D Fourier transform yields the depth-independent narrow beamwidth for the spherical transducer with a large aperture that is moving along two Cartesian coordinates x and y. It is thus shown that it is possible to use very high frequencies.

VI. ACKNOWLEDGEMENTS

This work has been partly supported by CRDF (USA) RP2-2104 and by the RFFI (Russia) N02-01-01087.

VII. REFERENCES

[1] C. Passmann and H. Ermert, “A 100 MHz Ultrasound Imaging System for Dermatologic and Ophthalmologic Diagnostics”, IEEE Trans. Ultrason., Ferroelect., Freq. Contr., vol. 43, pp. 545-552, July 1996.

[2] Z. M. Benenson, A. B. Elizarov, T. V. Yakovleva, W. D. O’Brien, Jr., “Approach to 3D Ultrasound High resolution Imaging Based upon Fourier Transform”, IEEE Trans. Ultrason., Ferroelectt., Freq. Contr., in press.